

# Fundamental limits on the rate of bacterial cell division

<sup>3</sup> Nathan M. Belliveau<sup>†, 1</sup>, Griffin Chure<sup>†, 2, 3</sup>, Christina L. Hueschen<sup>4</sup>, Hernan G.  
<sup>4</sup> Garcia<sup>5</sup>, Jané Kondev<sup>6</sup>, Daniel S. Fisher<sup>7</sup>, Julie Theriot<sup>1, 2, 8</sup>, Rob Phillips<sup>1, 2, 9, \*</sup>

\*For correspondence:

<sup>†</sup>These authors contributed equally to this work

<sup>5</sup> <sup>1</sup>Department of Biology, University of Washington, Seattle, WA, USA; <sup>2</sup>Division of  
<sup>6</sup> Biology and Biological Engineering, California Institute of Technology, Pasadena, CA,  
<sup>7</sup> USA; <sup>3</sup>Department of Applied Physics, California Institute of Technology, Pasadena, CA,  
<sup>8</sup> USA; <sup>4</sup>Department of Chemical Engineering, Stanford University, Stanford, CA, USA;  
<sup>9</sup> <sup>5</sup>Department of Molecular Cell Biology and Department of Physics, University of  
<sup>10</sup> California Berkeley, Berkeley, CA, USA; <sup>6</sup>Department of Physics, Brandeis University,  
<sup>11</sup> Waltham, MA, USA; <sup>7</sup>Department of Applied Physics, Stanford University, Stanford, CA,  
<sup>12</sup> USA; <sup>8</sup>Allen Institute for Cell Science, Seattle, WA, USA; <sup>9</sup>Department of Physics,  
<sup>13</sup> California Institute of Technology, Pasadena, CA, USA; \*Contributed equally

<sup>14</sup> 

---

## 15 Abstract

<sup>16</sup> 

---

## 17 Introduction

<sup>18</sup> The range of bacterial growth rates can be enormous. In natural environments, some microbial  
<sup>19</sup> organisms might double only once per year, whereas in comfortable laboratory conditions growth  
<sup>20</sup> can be rapid with several divisions per hour. This remarkable diversity illustrates the intimate re-  
<sup>21</sup> lationship between environmental conditions and the rates at which cells convert nutrients into  
<sup>22</sup> new cellular material. This relationship between the environment and cellular growth rate has re-  
<sup>23</sup> mained a major topic of inquiry in bacterial physiology for over a century (?). In 1958, Schaecter,  
<sup>24</sup> Malløe, and Kjeldgaard reported the discovery of a logarithmic relationship between the total cel-  
<sup>25</sup> lular protein content and the cellular growth rate, revealing a fundamental relationship between  
<sup>26</sup> the environment and the composition of the intracellular milieu (?).

<sup>27</sup> Over the past decade, a remarkable body of work has reexamined this relationship with single-  
<sup>28</sup> cell and single-protein resolution using modern methods of video microscopy (??) and through  
<sup>29</sup> advances in mass spectrometry and sequencing technologies (??). This has permitted quantitative  
<sup>30</sup> insight into how bacteria like *E. coli* allocate their cellular resources under nutrient-limitation, and  
<sup>31</sup> following genomic and pharmacological perturbations (??). This body of experimental data places  
<sup>32</sup> us in the auspicious position to explore how the abundance of essential protein complexes are  
<sup>33</sup> related to the growth rate of the population and interrogate what biological processes may set the  
<sup>34</sup> speed limit of bacterial growth.

<sup>35</sup> In this work, we seek to leverage a collection of proteomic data sets of *Escherichia coli* across  
<sup>36</sup> 31 growth conditions (?????) to quantitatively explore what biological processes may set the speed  
<sup>37</sup> limit of bacterial growth. Broadly speaking, we entertain several classes of hypotheses as are il-  
<sup>38</sup> lustrated in *Figure 1*. First, we consider potential limits on the transport of nutrients into the cell.  
<sup>39</sup> We address this hypothesis by performing an order-of-magnitude estimate for how many carbon  
<sup>40</sup> atoms needed to facilitate this requirement given a 6000 second division time. As a second hy-  
<sup>41</sup> pothesis, we consider the possibility that there exists a fundamental limit on how quickly the cell

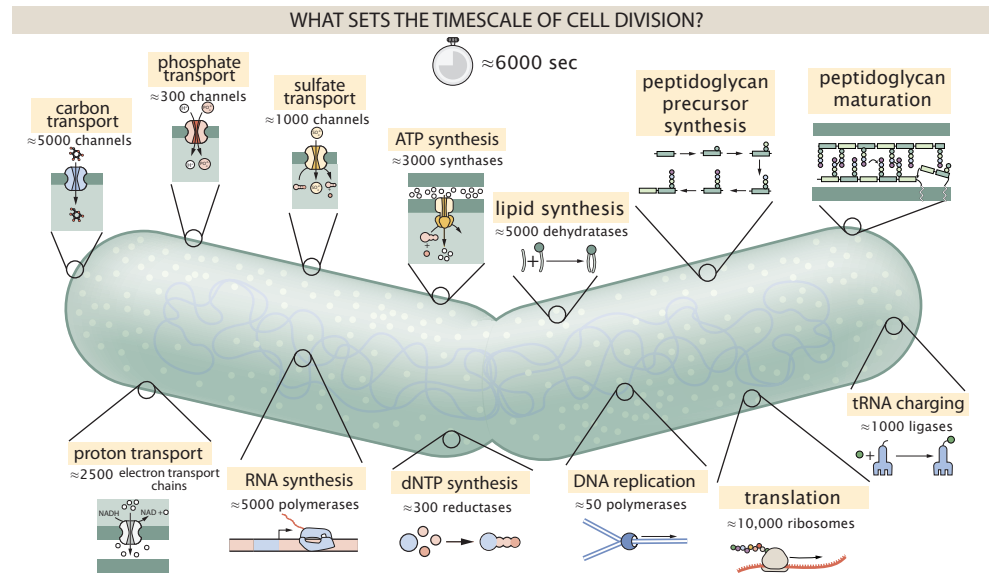


**Figure 1. Transport and synthesis processes necessary for cell division.** We consider an array of processes necessary for a cell to double its molecular components. Such processes include the transport of carbon across the cell membrane, the production of ATP, and fundamental processes of the central dogma namely RNA, DNA, and protein synthesis. A schematic of each synthetic or transport category is shown with an estimate of the rate per macromolecular complex. In this work, we consider a standard bacterial division time of  $\approx 6000$  sec.

42 can generate ATP. We approach this hypothesis from two angles, considering how many ATP syn-  
 43 thase complexes must be needed to churn out enough ATP to power protein translation followed  
 44 by an estimation of how many electron transport complexes must be present to maintain the pro-  
 45 ton motive force. Our third and final class of hypotheses centers on the synthesis of a variety of  
 46 biomolecules. Our focus is primarily on the stages of the central dogma as we estimate the number  
 47 of protein complexes needed for DNA replication, transcription, and protein translation.

48 With estimates in hand for each of these processes, we turn to our collection of data sets to  
 49 assess the accuracy of our estimates. In broad terms, we find that the majority of our estimates are  
 50 in line with experimental observations, with protein copy numbers apparently well-tuned for the  
 51 task of cell doubling. This allows us to systematically scratch off the hypotheses diagrammed in **Fig-**  
**52 ure 1** as setting possible speed limits. Ultimately, we find that protein translation (particularly the  
 53 generation of new ribosomes) acts as 1) a rate limiting step for the *fastest* bacterial division, and  
 54 2) the major determinant of bacterial growth across all nutrient conditions we have considered  
 55 under steady state, exponential growth. This perspective is in line with the linear correlation ob-  
 56 served between growth rate and ribosomal content (usually quantified through the ratio of RNA to  
 57 protein) for fast growing cells (?), but suggests a more prominent role for ribosomes in setting the  
 58 doubling time across all conditions of nutrient limitation. Here we again leverage the quantitative  
 59 nature of this data set and present a quantitative model of the relationship between the fraction  
 60 of the proteome devoted to ribosomes and the speed limit of translation, revealing a fundamental  
 61 tradeoff between the translation capacity of the ribosome pool and the maximal growth rate.

## 62 Nutrient Transport

63 In order to build new cellular mass, the molecular and elemental building blocks must be scaven-  
 64 enged from the environment in different forms. Carbon, for example, is acquired via the transport  
 65 of carbohydrates and sugar alcohols with some carbon sources receiving preferential treatment  
 66 in their consumption (?). Phosphorus, sulfur, and nitrogen, on the other hand, are harvested pri-  
 67 marily in the forms of inorganic salts, namely phosphate, sulfate, and ammonia (??????). All of

68 these compounds have different permeabilities across the cell membrane and most require some  
 69 energetic investment either via ATP hydrolysis or through the proton electrochemical gradient to  
 70 bring the material across the hydrophobic cell membrane. Given the diversity of biological trans-  
 71 port mechanisms and the vast number of inputs needed to build a cell, we begin by considering  
 72 transport of elemental requirements as a possible rate-limiting step of bacterial cell division.

73 The elemental composition of *E. coli* has received much quantitative attention over the past  
 74 half century (????), providing us with a starting point for estimating the copy numbers of various  
 75 transporters. While there is some variability in the exact elemental percentages (with different  
 76 uncertainties), we can estimate that the dry mass of a typical *E. coli* cell is  $\approx$  45% carbon (BNID:  
 77 100649, ?),  $\approx$  15% nitrogen (BNID: 106666, ?),  $\approx$  3% phosphorus (BNID: 100653, ?), and 1% sulfur  
 78 (BNID: 100655, ?). In the coming paragraphs, we will examine how many transporters and/or chan-  
 79 nels must be present to maintain these elemental compositions with a moderate doubling time of  
 80 6,000 s.

### 81 Carbon Transport

82 We begin with the most abundant element by mass, carbon. Using  $\approx$  0.3 pg as the typical *E. coli* dry  
 83 mass (BNID: 103904, ?), we estimate that  $\approx$   $10^{10}$  carbon atoms must be brought into the cell in or-  
 84 der to double all of the carbon-containing molecules (*Figure 2(A, top)*). Typical laboratory growth  
 85 conditions, such as those explored in the aforementioned proteomic data sets, provide carbon  
 86 as single class of sugar such as glucose, galactose, or xylose to name a few. *E. coli* has evolved  
 87 myriad mechanisms by which these sugars can be transported across the cell membrane. One  
 88 such mechanism of transport is via the PTS system which is a highly modular system capable of  
 89 transporting a diverse range of sugars (?). The glucose-specific component of this system trans-  
 90 ports  $\approx$  200 glucose molecules per second per channel (BNID: 114686, ?). Making the assumption  
 91 that this is a typical sugar transport rate, coupled with the need to transport  $10^{10}$  carbon atoms,  
 92 we arrive at the conclusion that on the order of 1,000 transporters must be expressed in order  
 93 to bring in enough carbon atoms to divide in 6,000 s, diagrammed in the top panel of *Figure 2(A)*.  
 94 This estimate, along with the observed average number of carbohydrate transporters present in  
 95 the proteomic data sets (????), is shown in *Figure 2(A)*. While we estimate 1,000 transporters are  
 96 needed, the data reveals that at a division time of  $\approx$  6,000 s there is nearly a ten-fold excess of trans-  
 97 porters. Furthermore, the data illustrates that the average number of carbohydrate transporters  
 98 present is largely-growth rate independent.

99 The estimate presented in *Figure 2(A)* neglects any specifics of the regulation of carbon trans-  
 100 port system and presents a data-averaged view of how many carbohydrate transporters are present  
 101 on average. Using the diverse array of growth conditions explored in the proteomic data sets, we  
 102 can explore how individual carbon transport systems depend on the population growth rate. In  
 103 *Figure 2(B)*, we show the total number of carbohydrate transporters specific to different carbon  
 104 sources. A striking observation, shown in the top-left plot of *Figure 2(B)*, is the constancy in the  
 105 expression of the glucose-specific transport systems (the PtsG enzyme of the PTS system and the  
 106 glucose-transporting ManXYZ complex). Additionally, we note that the total number of glucose-  
 107 specific transporters is tightly distributed  $\approx$   $10^4$  per cell, an order of magnitude beyond the esti-  
 108 mate shown in *Figure 2(A)*. This illustrates that *E. coli* maintains a substantial number of complexes  
 109 present for transporting glucose which is known to be the preferential carbon source (??).

110 It is now understood that a large number of metabolic operons are regulated with dual-input  
 111 logic gates that are only expressed when glucose concentrations are low (mediated by cyclic-AMP  
 112 receptor protein CRP) and the concentration of other carbon sources are elevated (??). A famed  
 113 example of such dual-input regulatory logic is in the regulation of the *lac* operon which is only  
 114 natively activated in the absence of glucose and the presence of allolactose, an intermediate in  
 115 lactose metabolism (?), though we now know of many other such examples (??). This illustrates  
 116 that once glucose is depleted from the environment, cells have a means to dramatically increase  
 117 the abundance of the specific transporter needed to digest the next sugar that is present. Several

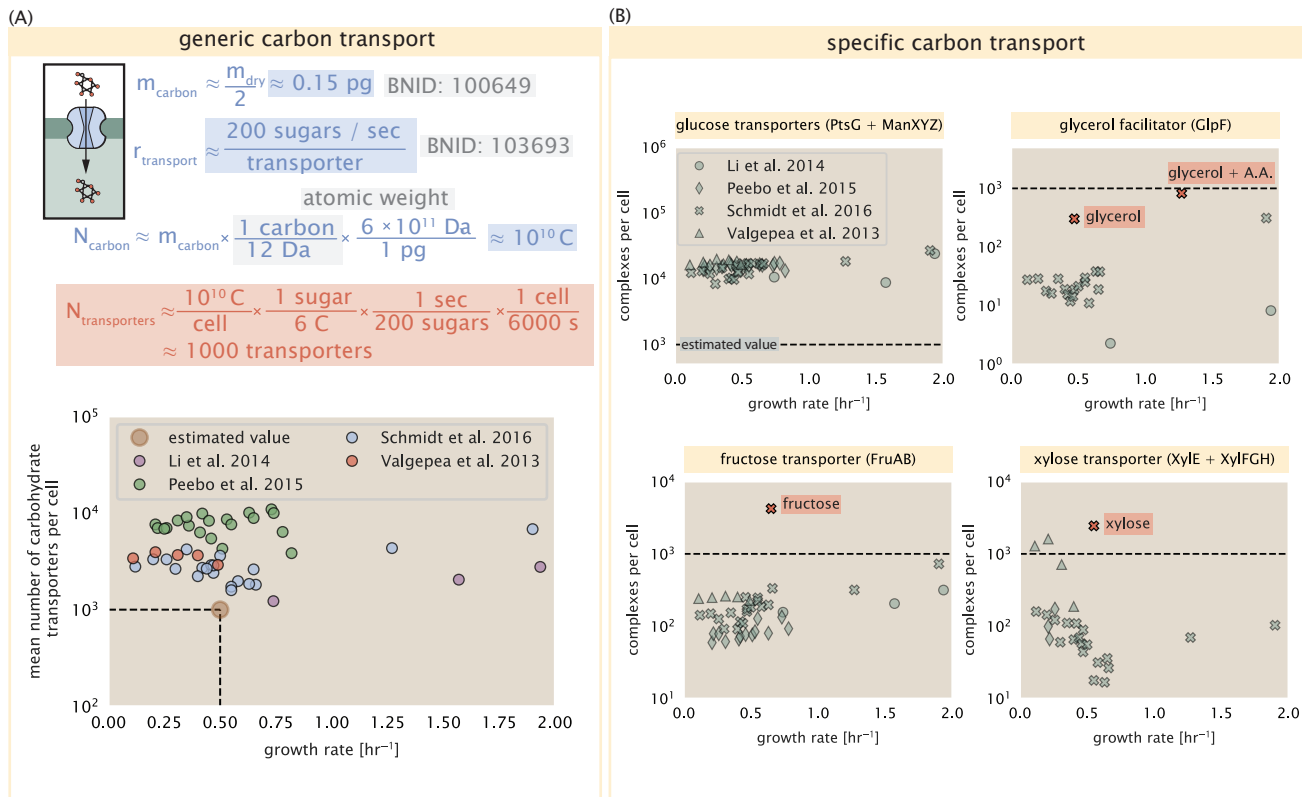


**Figure 2. The abundance of carbon transport systems across growth rates.** (A) A simple estimate for the minimum number of generic carbohydrate transport systems (top) assumes  $\approx 10^{10}$  C are needed to complete division, each transported sugar contains  $\approx 6$  C, and each transporter conducts sugar molecules at a rate of  $\approx 200$  per second. Bottom plot shows the estimated number of transporters needed at a growth rate of  $\approx 0.5$  per hr (light-brown point and dashed lines). Colored points correspond to the mean number of carbohydrate transporters for different growth conditions across different published datasets. (B) The abundance of various specific carbon transport systems plotted as a function of the population growth rate. Red points and red-highlighted text indicate conditions in which the only source of carbon in the growth medium induces expression of the transport system.

examples of induced expression of a specific carbon-source transporters are shown in **Figure 2(B)**. Points colored in red (labeled by red text-boxes) correspond to growth conditions in which the specific carbon source (glycerol, xylose, or fructose) is present. These plots show that, in the absence of the particular carbon source, expression of the transporters is maintained on the order of  $\sim 10^2$  per cell. However, when induced, the transporters become highly-expressed and are present on the order of  $\sim 10^4$  per cell, which exceeds the generic estimate given in **Figure 2(A)**. Together, this generic estimation and the specific examples of induced expression suggest that transport of carbon across the cell membrane, while critical for growth, is not the rate-limiting step of cell division.

In the context of speeding up growth, one additional limitation is the fact that the cell's inner membrane is occupied by a multitude of other membrane proteins. Considering a rule-of-thumb for the surface area of *E. coli* of about  $6 \mu\text{m}^2$  (BNID: 101792, ?), we expect an areal density for 1,000 transporters to be approximately 200 transporters/ $\mu\text{m}^2$ . For a glucose transporter occupying about  $50 \text{ nm}^2/\text{dimer}$ , this amounts to about only 1 percent of the total inner membrane (?). In addition, bacterial cell membranes typically have densities of  $10^5$  proteins// $\mu\text{m}^2$  (?), implying that the cell could accommodate more transporters if it were rate limiting.

### **133 Phosphorus and Sulfur Transport**

We now turn our attention towards other essential elements, namely phosphorus and sulfur. Phosphorus is critical to the cellular energy economy in the form of high-energy phosphodiester bonds making up DNA, RNA, and the NTP energy pool as well as playing a critical role in the post-translational modification of proteins and defining the polar-heads of lipids. In total, phosphorus makes up  $\approx 3\%$  of the cellular dry mass which in typical experimental conditions is in the form of inorganic phosphate. The cell membrane has remarkably low permeability to this highly-charged and critical molecule, therefore requiring the expression of active transport systems. In *E. coli*, the proton electrochemical gradient across the inner membrane is leveraged to transport inorganic phosphate into the cell (?). Proton-solute symporters are widespread in *E. coli* (??) and can have rapid transport rates of 50 molecules per second for sugars and other solutes (BNID: 103159; 111777, ?). In *E. coli* the PitA phosphate transport system has been shown to very tightly coupled with the proton electrochemical gradient with a 1:1 proton:phosphate stoichiometric ratio (??). Illustrated in **Figure 3(A)**, we can estimate that  $\approx 300$  phosphate transporters are necessary to maintain an  $\approx 3\%$  dry mass with a 6,000 s division time. This estimate is again satisfied when we examine the observed copy numbers of PitA in proteomic data sets (plot in **Figure 3(A)**). While our estimate is very much in line with the observed numbers, we emphasize that this is likely a slight over estimate of the number of transporters needed as there are other phosphorous scavenging systems, such as the ATP-dependent phosphate transporter Pst system which we have neglected.

Satisfied that there are a sufficient number of phosphate transporters present in the cell, we now turn sulfur transport as another potentially rate limiting process. Similar to phosphate, sulfate is highly-charged and not particularly membrane permeable, requiring active transport. While there exists a H+/sulfate symporter in *E. coli*, it is in relatively low abundance and is not well characterized (?). Sulfate is predominantly acquired via the ATP-dependent ABC transporter CysUWA system which also plays an important role in selenium transport (??). While specific kinetic details of this transport system are not readily available, generic ATP transport systems in prokaryotes are on the order of 1 to 10 molecules per second (BNID: 109035, ?). Combining this generic transport rate, measurement of sulfur comprising 1% of dry mass, and a 6,000 second division time yields an estimate of  $\approx 1000$  CysUWA complexes per cell (**Figure 3(B)**). Once again, this estimate is in notable agreement with proteomic data sets, suggesting that there are sufficient transporters present to acquire the necessary sulfur. In a similar spirit of our estimate of phosphorus transport, we emphasize that this is likely an overestimate of the number of necessary transporters as we have neglected other sulfur scavenging systems that are in lower abundance.

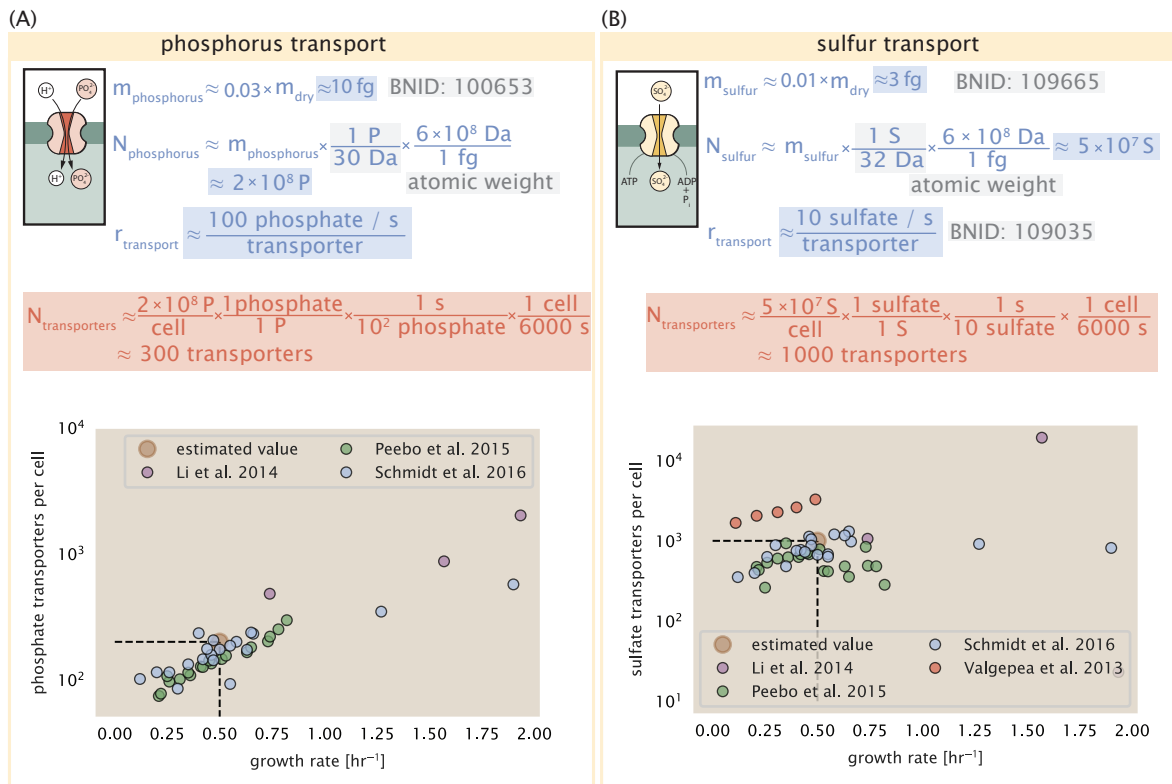


**Figure 3. Estimates and measurements of phosphate and sulfate transport systems as a function of growth rate.** (A) Estimate for the number of PitA phosphate transport systems needed to maintain a 3% phosphorus *E. coli* dry mass. Points in plot correspond to the total number of PitA transporters per cell. (B) Estimate of the number of CysUWA complexes necessary to maintain a 1% sulfur *E. coli* dry mass. Points in plot correspond to average number of CysUWA transporter complexes that can be formed given the transporter stoichiometry [CysA]<sub>2</sub>[CysU][CysW][Sbp/CysP].

**166 Nitrogen Transport**

167 Finally, we turn to nitrogen transport as the last remaining transport system highlighted in **Figure 1**. Unlike phosphate, sulfate, and various sugar molecules, nitrogen in the form of ammonia  
 168 can readily diffuse across the cell membrane and has a permeability on par with water ( $\approx 10^5$  nm/s,  
 169 BNID:110824 ?). In particularly nitrogen-poor conditions, *E. coli* expresses a transporter (AmtB)  
 170 which appears to aid in nitrogen assimilation, though the mechanism and kinetic details of trans-  
 171 port is still a matter of debate (??). Beyond ammonia, another plentiful source of nitrogen come  
 172 in the form of glutamate, which has its own complex metabolism and scavenging pathways. How-  
 173 ever, nitrogen is plentiful in the growth conditions examined in this work, permitting us to neglect  
 174 nitrogen transport as a potential rate limiting process in cell division.

**176 Energy Production**

177 While the transport of nutrients is required to build new cell mass, the metabolic pathways in-  
 178 volved in assimilation both consumes and generates energy in the form of NTPs. The high-energy  
 179 phosphodiester bonds of (primarily) ATP power a variety of cellular processes that drive biological  
 180 systems away from thermodynamic equilibrium. Our next class of estimates consider the energy  
 181 budget of a dividing cell in terms of the synthesis of ATP from ADP and inorganic phosphate as well  
 182 as maintenance of the electrochemical proton gradient which powers it.

**183 ATP Synthesis**

184 Hydrolysis of the terminal phosphodiester bond of ATP forming ADP and an inorganic phosphate is  
 185 a kinetic driving force in a wide array of biochemical reactions. One such reaction is the formation  
 186 of peptide bonds during translation which requires  $\approx 2$  ATPs for the charging of an amino acid  
 187 to the tRNA and  $\approx 2$  ATP equivalents for the formation of the peptide bond between amino acids.  
 188 Together, these energetic costs consume  $\approx 80\%$  of the cells ATP budget (BNID: 107782; 106158;  
 189 101637; 111918, ?). The pool of ATP is produced by the F<sub>1</sub>-F<sub>0</sub> ATP synthase – a membrane-bound  
 190 rotary motor which under ideal conditions can yield  $\approx 300$  ATP per second (BNID: 114701; ??).

191 To estimate the total number of ATP equivalents consumed during a cell cycle, we will make  
 192 the approximation that there are  $\approx 3 \times 10^6$  proteins per cell with an average protein length of  $\approx$   
 193 300 peptide bonds (BNID: 115702; 108986; 104877, ?). Taking these values together, we estimate  
 194 that the typical *E. coli* cell consumes  $\approx 5 \times 10^9$  ATP per cell cycle on protein synthesis alone and  
 195  $\approx 6 \times 10^9$  ATP in total. Assuming that the ATP synthases are operating at their fastest possible rate,  
 196  $\approx 3000$  ATP synthases are needed to keep up with the energy demands of the cell. This estimate  
 197 and a comparison with the data are shown in **Figure 4 (A)**. Despite our assumption of maximal ATP  
 198 production rate per synthase and approximation of all NTP consuming reactions being the same  
 199 as ATP, we find that an estimate of a few thousand complete synthases per cell to agree well with  
 200 the experimental data.

**201 Generating the Proton Electrochemical Gradient**

202 In order to produce ATP, the F<sub>1</sub>-F<sub>0</sub> ATP synthase itself must consume energy. Rather than burning  
 203 through its own product, this intricate macromolecular machine has evolved to exploit the elec-  
 204 trochemical potential established across the inner membrane through cellular respiration. This  
 205 electrochemical gradient is manifest by the pumping of protons into the intermembrane space via  
 206 the electron transport chains as they reduce NADH. In *E. coli*, this potential difference is  $\approx -200$   
 207 mV (BNID: 102120, ?). As estimated in the supporting information, this potential difference is gen-  
 208 erated by maintaining  $\approx 2 \times 10^4$  protons in the intermembrane space.

209 However, the constant rotation of the ATP synthases would rapidly abolish this potential differ-  
 210 ence if it were not being actively maintained. To undergo a complete rotation (and produce a single  
 211 ATP), the F<sub>1</sub>-F<sub>0</sub> ATP synthase must shuttle  $\approx 4$  protons across the membrane into the cytosol (BNID:  
 212 103390, ?). With  $\approx 3000$  ATP synthases each generating 300 ATP per second, the  $2 \times 10^4$  protons

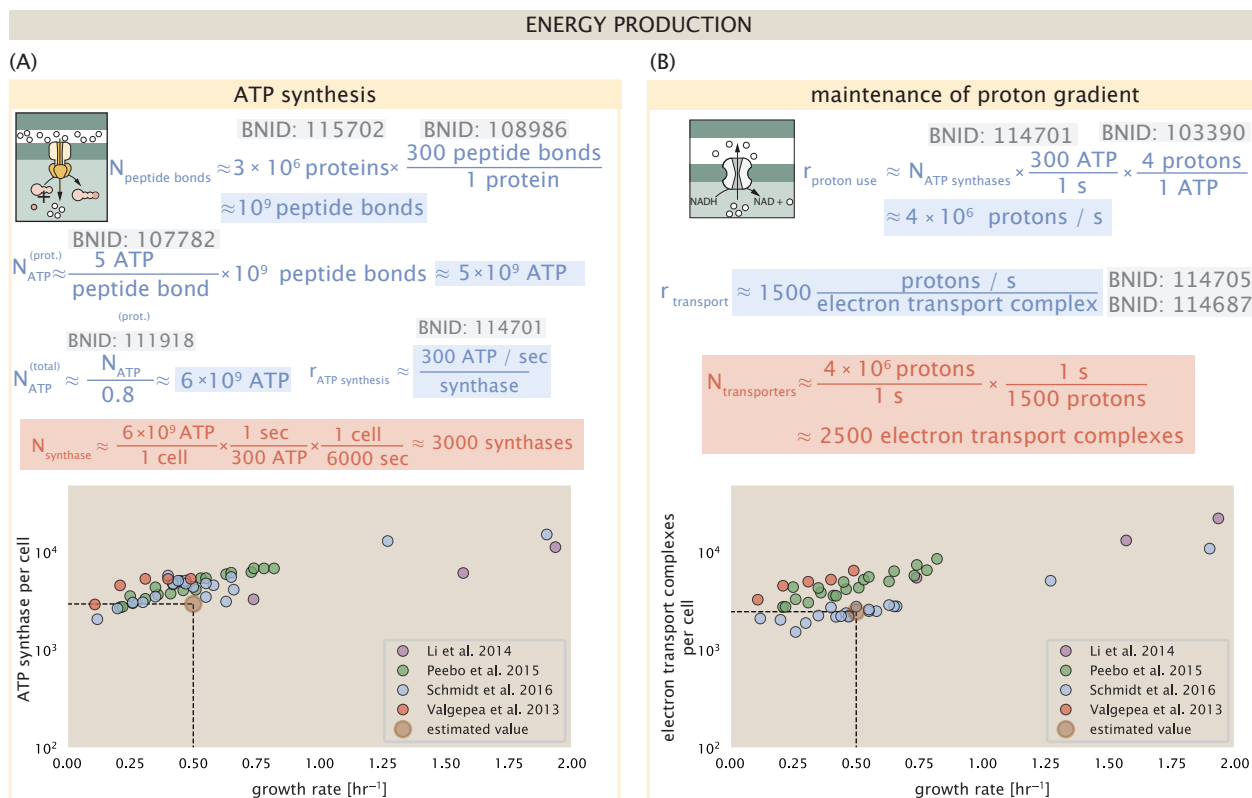


**Figure 4. The abundance of  $F_1$ - $F_0$  ATP synthases and electron transport chain complexes as a function of growth rate.** (A) Estimate of the number of  $F_1$ - $F_0$  ATP synthase complexes needed accommodate peptide bond formation and other NTP dependent processes. Points in plot correspond to the mean number of complete  $F_1$ - $F_0$  ATP synthase complexes that can be formed given proteomic measurements and the subunit stoichiometry  $[AtpE]_{10}[AtpF]_2[AtpB][AtpC][AtpH][AtpA]_3[AtpG][AtpD]_3$ . (B) Estimate of the number of electron transport chain complexes needed to maintain a membrane potential of  $\sim 200$  mV given estimate of number of  $F_1$ - $F_0$  ATP synthases from (A). Points in plot correspond to the average number of complexes identified as being involved in aerobic respiration by the Gene Ontology identifier GO:0019646 that could be formed given proteomic observations. These complexes include cytochromes *bd1* ( $[CydA][CydB][CydX][CydH]$ ), *bdII* ( $[AppC][AppB]$ ), *bo3*, ( $[CyoD][CyoA][CyoB][CyoC]$ ) and NADH:quinone oxireducase I ( $[NuoA][NuoH][NuoJ][NuoK][NuoL][NuoM][NuoN][NuoB][NuoC][NuoE][NuoF][NuoG][NuoI]$ ) and II ( $[Ndh]$ ).

213 establishing the 200 mV potential would be consumed in only a few milliseconds. This brings us to our  
 214 next estimate: how many electron transport complexes are needed to support the consumption  
 215 rate of the ATP synthases?

216 The electrochemistry of the electron transport complexes of *E. coli* have been the subject of  
 217 intense biochemical and biophysical study over the past half century (????). A recent work (?) ex-  
 218 amined the respiratory capacity of the *E. coli* electron transport complexes using structural and  
 219 biochemical data, revealing that each electron transport chain rapidly pumps protons into the in-  
 220 termembrane space at a clip of  $\approx 1500$  protons per second (BNID: 114704; 114687, ?). Using our  
 221 estimate of the number of ATP synthases required per cell (Figure 4(A)), coupled with these re-  
 222 cent measurements, we estimate that  $\approx 4 \times 10^6$  protons per second diet of the cellular ATP synthases. This estimate is in  
 223 agreement with the number of complexes identified in the proteomic datasets (plot in Figure 4(B)).

### 225 Energy Production in a Crowded Membrane.

226 For each protein considered so far, the data shows that in general their numbers increase with  
 227 growth rate. This is in part a consequence of the increase in cell length and width at that is com-  
 228 mon to many rod-shaped bacteria at faster growth rates (??). For the particular case of *E. coli*, the

229 total cellular protein and cell size increase logarithmically with growth rate (??). Indeed, this is one  
 230 reason why we have considered only a single, common growth condition across all our estimates  
 231 so far. Such a scaling will require that the total number of proteins and net demand on resources  
 232 also grow in proportion to the increase in cell size divided by the cell's doubling time. Recall how-  
 233 ever that each transport process, as well as the ATP production via respiration, is performed at the  
 234 bacterial membrane. This means that their maximum productivity can only increase in proportion  
 235 to the cell's surface area divided by the cell doubling time. This difference in scaling would vary in  
 236 proportion to the surface area-to-volume (S/V) ratio.

237 While we found that there was more than sufficient membrane real estate for carbon intake in  
 238 our earlier estimate, the total number of ATP synthases and electron chain transport complexes  
 239 both exhibit a clear increase in copy number with growth rate, reaching in excess of  $10^4$  copies per  
 240 cell (**Figure 4**). Here we consider the consequences of this S/V ratio scaling in more detail.

241 In our estimate of ATP production above we found that a cell demands about  $6 \times 10^9$  ATP or  $10^6$   
 242 ATP/s. With a cell volume of roughly 1 fL, this corresponds to about  $2 \times 10^{10}$  ATP per fL of cell volume,  
 243 in line with previous estimates (??). In **Figure 5 (A)** we plot this ATP demand as a function of the  
 244 S/V ratio in green, where we have considered a range of cell shapes from spherical to rod-shaped  
 245 with an aspect ratio (length/width) equal to 4 (See appendix for calculations of cell volume and  
 246 surface area). In order to consider the maximum power that could be produced, we consider the  
 247 amount of ATP that can generated by a membrane filled with ATP synthase and electron transport  
 248 complexes, which provides a maximal production of about 3 ATP / (nm<sup>2</sup>·s) (?). This is shown in  
 249 red in **Figure 5(A)**, which shows that at least for the growth rates observed, the energy demand is  
 250 roughly an order of magnitude less. Interestingly, ? also found that ATP production by respiration  
 251 is less efficient than by fermentation per membrane area occupied due to the additional proteins  
 252 of the electron transport chain. This suggests that even under anaerobic growth, there will be  
 253 sufficient membrane space for ATP production in general.

254 While this serves to highlight the diminishing capacity to provide resources to grow if the cell  
 255 increases in size (and its S/V decreases), the blue region in **Figure 5(A)** represents a somewhat un-  
 256 achievable limit since the inner membrane must also include other proteins such as those required  
 257 for lipid and membrane synthesis. To gain insight, we used the proteomic data to look at the distri-  
 258 bution of proteins on the inner membrane. Here we use Gene Ontology (GO) annotations (??) to  
 259 identify all proteins embedded or peripheral to the inner membrane (GO term: 0005886). Those  
 260 associated but not membrane-bound include proteins like MreB and FtsZ, that traverse the inner  
 261 membrane by treadmilling and must nonetheless be considered as a vital component occupying  
 262 space on the membrane. In **Figure 5 (B)**, we find that the total protein mass per  $\mu\text{m}^2$  is relatively  
 263 constant with growth rate. Interestingly, when we consider the distribution of proteins grouped  
 264 by their Clusters of Orthologous Groups (COG) (?), the relative abundance for those in metabolism  
 265 (including ATP synthesis via respiration) is also relatively constant.

## 266 **Synthesis of the Cell Wall and lipid membrane.**

267 [To be completed.]

## 268 **Function of the Central Dogma**

269 Up to this point, we have considered a variety of transport and biosynthetic processes that are  
 270 critical to acquiring and generating new cell mass. While there are of course many other metabolic  
 271 processes we could consider and perform estimates of (such as the components of fermentative  
 272 versus aerobic respiration), we now turn our focus to some of the most central processes which  
 273 *must* be undertaken irrespective of the growth conditions – the processes of the central dogma.

## 274 **DNA**

275 Most bacteria (including *E. coli*) harbor a single, circular chromosome and can have extra-chromosomal  
 276 plasmids ~ 100 kbp in length. We will focus our quantitative thinking solely on the chromosome

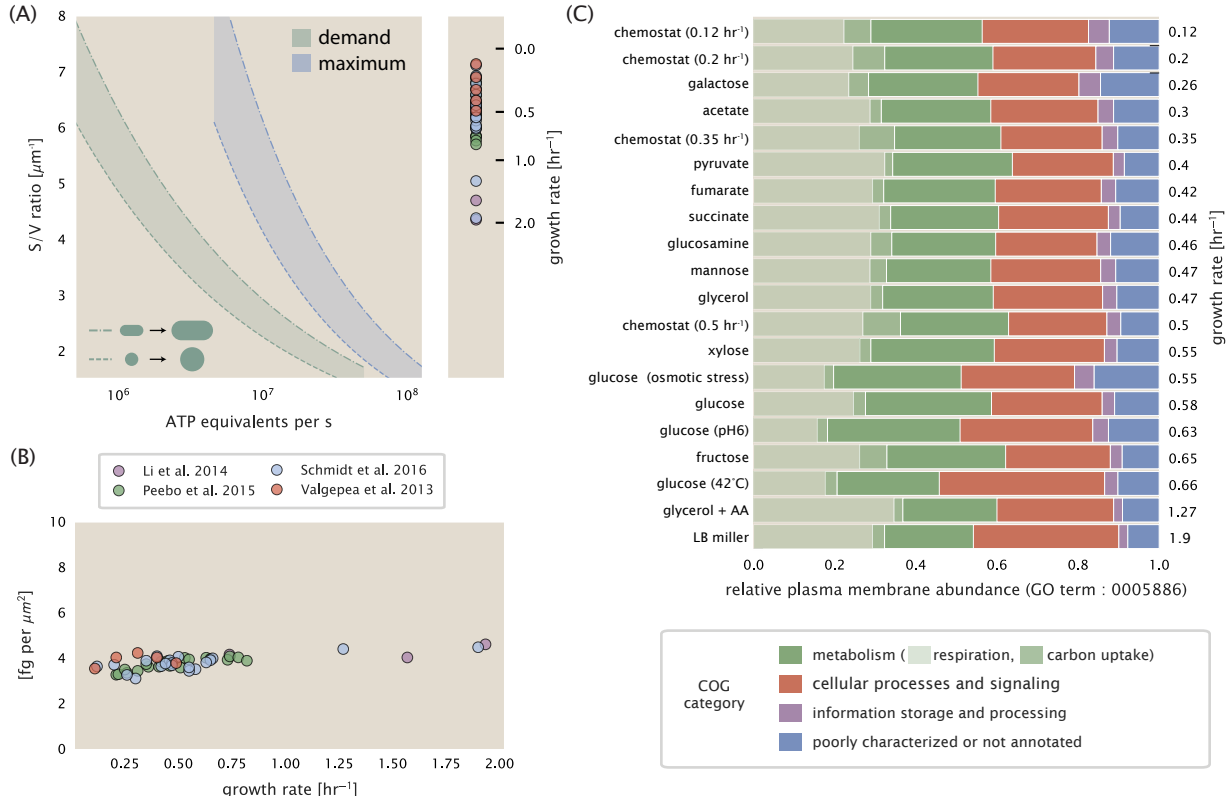


**Figure 5. Influence of cell size and S/V ratio on ATP production and inner membrane composition.** (A) Scaling of ATP demand and maximum ATP production as a function of S/V ratio. Cell volumes of 0.5 fL to 50 fL were considered, with the dashed (—) line corresponding to a sphere and the dash-dot line (---) reflecting a rod-shaped bacterium like *E. coli* with aspect ratio (length / width) of 0.4. Approximately 50% of the bacterial inner membrane is assumed to be protein, with the remainder lipid. (B) Total protein mass calculated for proteins with inner membrane annotation (GO term: 0005886). (C) Relative protein abundances by mass based on COG annotation. Metabolic proteins are further separated into respiration ( $F_1$ - $F_0$  ATP synthase, NADH dehydrogenase I, succinate:quinone oxidoreductase, cytochrome  $b_{o3}$  ubiquinol oxidase, cytochrome  $bd$ -I ubiquinol oxidase) and carbohydrate transport (GO term: GO:0008643). Note that the elongation factor EF-Tu can also associate with the inner membrane, but was excluded in this analysis due to its high relative abundance (roughly identical to the total mass shown in part (B)).

277 of *E. coli* which harbors  $\approx$  5000 genes and  $\approx$   $5 \times 10^6$  base pairs. To successfully divide and produce  
 278 viable progeny, this chromosome must be faithfully replicated and segregated into each nascent  
 279 cell. We again rely on the near century of literature in molecular biology to provide some insight  
 280 towards the rates and mechanics of the replicative feat as well as the production of the replication  
 281 starting materials, dNTPs.

#### 282 dNTP synthesis

283 We begin our exploration of the DNA replicative processes by examining the production of the de-  
 284 oxyribonucleotide triphosphates (dNTPs). The four major dNTPS (dATP, dTTP, dCTP, and dGTP) are  
 285 synthesized *de novo* in separate pathways, requiring different building blocks. However, a critical  
 286 step present in all dNTP synthesis pathways is the conversion from ribonucleotide to deoxyribonu-  
 287 cleotide via the removal of the 3' hydroxyl group of the ribose ring (?). This reaction is mediated  
 288 by a class of enzymes termed ribonucleotide reductases, of which *E. coli* possesses two aerobically  
 289 active complexes (termed I and II) and a single anaerobically active enzyme. Due to their peculiar  
 290 formation of a radical intermediate, these enzymes have received much biochemical, kinetic, and  
 291 structural characterization. One such work (?) performed a detailed *in vitro* measurement of the  
 292 steady-state kinetic rates of these complexes, revealing a turnover rate of  $\approx$  10 per second.

293 Considering this reaction (mediated by the ribonucleotide reductase complexes I and II) is cen-  
 294 tral to synthesis of all dNTPS, it is reasonable to consider the abundance of these complexes as a  
 295 measure of the total dNTP production in *E. coli*. Illustrated schematically in **Figure 6 (A)**, we consider  
 296 the fact that to replicate the cell's genome, on the order of  $\approx$   $10^7$  dNTPs must be synthesized. As-  
 297 suming a production rate of 10 per second per ribonucleotide reductase complex and a cell division  
 298 time of 6000 seconds, we arrive at an estimate of  $\approx$  150 complexes are needed per cell. As shown  
 299 in the bottom panel of **Figure 6 (A)**, this estimate agrees with the experimental measurements of  
 300 these complexes abundances within  $\approx$  1/2 an order of magnitude.

301 Recent work has revealed that during replication, the ribonucleotide reductase complexes co-  
 302 alesce to form discrete foci colocalized with the DNA replisome complex (?). This is particularly  
 303 pronounced in environments where growth is slow, indicating that spatial organization and regu-  
 304 lation of the activity of the complexes plays an important role.

#### 305 DNA Replication

306 We now turn our focus towards the process of integration of the dNTP building blocks into the  
 307 replicated chromosome strand via the DNA polymerase enzymes. Replication of bacterial chromo-  
 308 somes is initiated at a single region of the chromosome termed the *oriC* locus at which a pair of DNA  
 309 polymerases bind and begin their high-fidelity replication of the genome in opposite directions. As-  
 310 suming equivalence between the two replication forks, this means that the two DNA polymerase  
 311 complexes (termed replisomes) meet at the midway point of the circular chromosome termed the  
 312 *ter* locus. This division of labor means The kinetics of the five types of DNA polymerases (I – V)  
 313 have been intensely studied, revealing that DNA polymerase III performs the high fidelity pro-  
 314 cessive replication of the genome with the other "accessory" polymerases playing auxiliary roles (?). *In*  
 315 *vitro* measurements have shown that DNA Polymerase III copies DNA at a rate of  $\approx$  600 nucleotides  
 316 per second (BNID: 104120, ?). Therefore, to replicate a single chromosome, two DNA polymerases  
 317 replicating at their maximal rate would copy the entire genome in  $\approx$  4000 s. Thus, with a division  
 318 time of 6000 s (our "typical" growth rate for the purposes of this work), there is sufficient time for  
 319 a pair of DNA polymerase III complexes to replicate the entire genome. However, this estimate  
 320 implies that 4000 s would be the upper-limit time scale for bacterial division which is at odds with  
 321 the familiar  $\approx$  1500 s doubling time of *E. coli* in rich medium.

322 It is known well known that *E. coli* can parallelize its DNA replication such that multiple chromo-  
 323 somes are being replicated at once. Recent work (?) has shown that the replicative timescale of  
 324 cell division can be massively parallelized where *E. coli* can have on the order of 10 - 12 replica-  
 325 tion forks at a given time. Thus, even in rapidly growing cultures, only a few polymerases ( $\approx$  10)

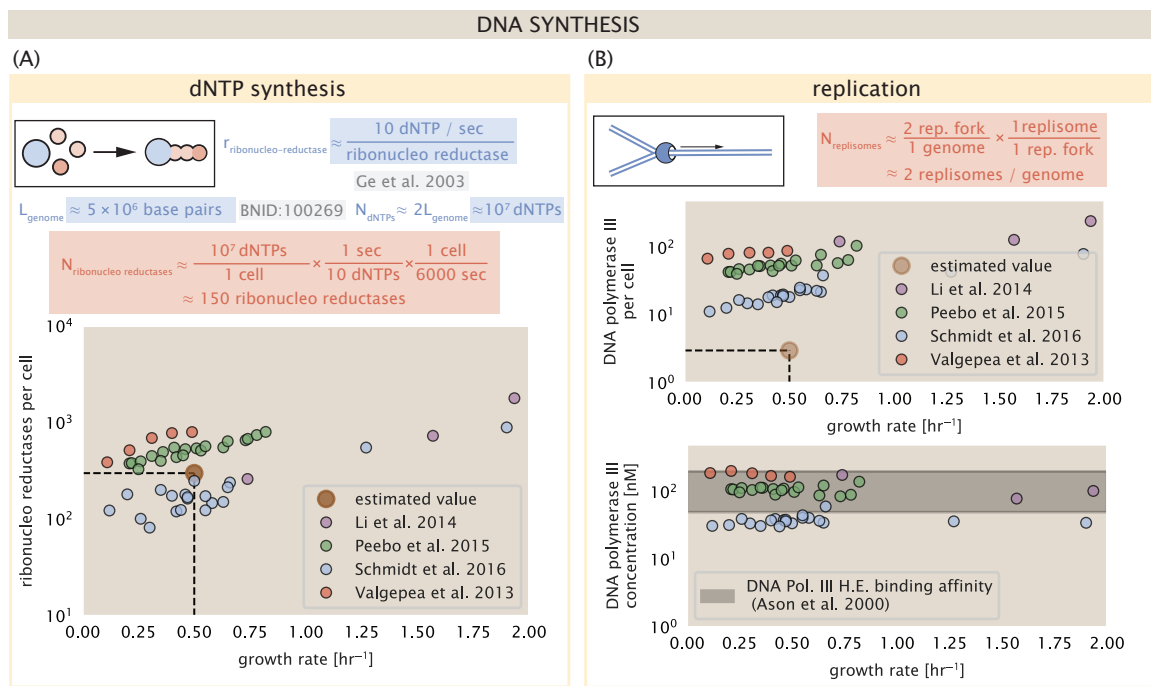


**Figure 6. Complex abundance estimates for dNTP synthesis and DNA replication.** (A) Estimate of the number of ribonucleotide reductase enzymes needed to facilitate the synthesis of  $\approx 10^7$  dNTPs over the course of a 6000 second generation time. Points in the plot correspond to the total number of ribonucleotide reductase I ( $[\text{NrdA}]_2[\text{NrdB}]_2$ ) and ribonucleotide reductase II ( $[\text{NrdE}]_2[\text{NrdF}]_2$ ) complexes. (B) An estimate for the minimum number of DNA polymerase holoenzyme complexes needed to facilitate replication of a single genome. Points in the top plot correspond to the total number of DNA polymerase III holoenzyme complexes ( $[\text{DnaE}]_3[\text{DnaQ}]_3[\text{HolE}]_3[\text{DnaX}]_5[\text{HolB}] [\text{HolA}][\text{DnaN}]_4[\text{HolC}]_4[\text{HolD}]_4$ ) per cell. Bottom plot shows the effective concentration of DNA polymerase III holoenzyme given cell volumes calculated from the growth rate as in ?.

326 are needed to replicate the chromosome. However, as shown in **Figure 6(B)**, DNA polymerase III is  
 327 nearly an order of magnitude more abundant. This discrepancy can be understood when  
 328 considering the binding affinities. The DNA polymerase III complex is highly processive, facilitated  
 329 by a strong affinity of the complex to the DNA. *In vitro* biochemical characterization has quantified  
 330 the  $K_D$  of DNA polymerase III holoenzyme to single-stranded and double-stranded DNA to be 50  
 331 and 200 nM, respectively (?). The bottom plot in **Figure 6 (B)** shows that the concentration of the  
 332 DNA polymerase III across all data sets and growth conditions is within this range. Thus, while  
 333 the copy number of the DNA polymerase III is in excess of the strict number required to replicate  
 334 the genome, the copy number is tuned such that the concentration is approximately equal to the  
 335 dissociation constant to the DNA. While the processes regulating the initiation of DNA replication  
 336 are complex and involve more than just the holoenzyme, these data indicate that the kinetics of  
 337 replication rather than the explicit copy number of the DNA polymerase III holoenzyme is the more  
 338 relevant feature of DNA replication to consider.

### 339 **RNA Synthesis**

340 With the machinery governing the replication of the genome accounted for, we now turn our atten-  
 341 tion to the next stage of the central dogma – the transcription of DNA to form RNA. We primarily  
 342 consider three major groupings of RNA, namely the RNA associated with ribosomes (rRNA), the  
 343 RNA encoding the amino-acid sequence of proteins (mRNA), and the RNA which links codon se-  
 344 quence to amino-acid identity during translation (tRNA). Despite the varied function of these RNA  
 345 species, they share a commonality in that they are transcribed from DNA via the action of RNA  
 346 polymerase. In the coming paragraphs, we will consider the synthesis of RNA as a rate limiting  
 347 step in bacterial division by estimating how many RNA polymerases must be present to synthesize  
 348 all necessary rRNA, mRNA, and tRNA.

#### 349 **rRNA**

350 We begin with an estimation of the number of RNA polymerases needed to synthesize the rRNA  
 351 that serve as catalytic and structural elements of the ribosome. Each ribosome contains three  
 352 rRNA molecules of lengths 120, 1542, and 2904 nucleotides (BNID: 108093, ?). Thus, each ribosome  
 353 consists of  $\approx$  4500 nucleotides. The *E. coli* RNA polymerase transcribes DNA to RNA at a rate of  $\approx$   
 354 40 nucleotides per second (BNID: 101904, ?). Thus, it takes a single RNA polymerase  $\approx$  100 s to  
 355 synthesize the RNA needed to form a functional ribosome. Therefore, in a 5000 s division time, a  
 356 single RNA polymerase transcribing rRNA at a time would result in only  $\approx$  50 functional ribosomal  
 357 rRNA units – far below the observed number of  $\approx$   $10^4$  ribosomes per cell.

358 Of course, there can be more than one RNA polymerase transcribing at any given time. To elu-  
 359 cidate the *maximum* number of rRNA units that can be synthesized given a single copy of each rRNA  
 360 gene, we will consider a hypothesis in which the rRNA operon is completely tiled with RNA poly-  
 361 merase. How many polymerase could in principle fit on the rRNA operon? *In vivo* measurements  
 362 of the kinetics of rRNA transcription have revealed that RNA polymerase are loaded onto the pro-  
 363 moter of an rRNA gene at a rate of  $\approx$  1 per second (BNID: 111997; 102362, ?). If RNA polymerases  
 364 are being constantly loaded on to the rRNA genes at this rate, then we can make the approximation  
 365 that  $\approx$  1 functional rRNA unit is synthesized per second. With a 5000 second division time, this hy-  
 366 pothesis leads to a maximal value of 5000 functional rRNA units, still undershooting the observed  
 367 number of  $10^4$  ribosomes per cell.

368 *E. coli* has evolved a clever mechanism to surpass this kinetic limit for the rate of rRNA produc-  
 369 tion. Rather than having only one copy of each rRNA gene, *E. coli* has seven copies of the operon  
 370 (BIND: 100352, ?) all of which are localized near the origin of replication (?). As fast growth requires  
 371 that multiple copies are being synthesized simultaneously, this means that the total number of  
 372 rRNA genes can be on the order of  $\approx$  10 – 30 at a given time (?). Using our standard time scale of  
 373 a 6000 second division time, we can make the lower-bound estimate that the typical cell will have  
 374 7 copies of the rRNA operon. Synthesizing one functional rRNA unit per second per operon, a total

375 of  $4 \times 10^4$  rRNA units can be synthesized, comfortably above the observed number of ribosomes  
 376 per cell.

377 How many RNA polymerases are then needed to constantly transcribe 7 copies of the rRNA  
 378 genes? We approach this estimate by considering the maximum number of RNA polymerases  
 379 can be tiling the rRNA genes with a loading rate of 1 per second and a transcription rate of 40 nu-  
 380 cleotides per second. Considering that a RNA polymerase has a physical footprint of approximately  
 381 40 nucleotides (BNID: 107873, ?), we can state that there is  $\approx 1$  RNA polymerase per 80 nucleotides.  
 382 With a total length of  $\approx 4500$  nucleotides per operon and 7 operons per well, the maximum num-  
 383 ber of RNA polymerases that can be transcribing rRNA at any given time is  $\approx 400$ , setting a lower  
 384 bound for the number of RNA polymerase required to make enough rRNA. As we will see in the  
 385 coming sections, the synthesis of rRNA is the dominant requirement of the RNA polymerase pool.

### 386 mRNA

387 To form a functional protein, all protein coding genes must first be transcribed from DNA to form  
 388 an mRNA molecule. While each protein requires an mRNA blueprint, many copies of the protein  
 389 can be synthesized from a single mRNA. Factors such as strength of the ribosomal binding site,  
 390 mRNA stability, and rare codon usage frequency dictate the number of proteins that can be made  
 391 from a single mRNA, ranging from  $10^1$  to  $10^4$  (BNID: 104186; 100196; 106254, ?). Computing the  
 392 geometric mean of this range yields  $\approx 1000$  proteins synthesized per mRNA, a value that emerges  
 393 from quantitative measurements of the number of proteins per cell ( $\approx 3 \times 10^6$ , BNID: 100088, ?)  
 394 and total number of mRNA per cell ( $\approx 3 \times 10^3$ , BNID: 100064, ?).

395 This estimation captures the *steady state* mRNA copy number, meaning that at any given time,  
 396 there will exist approximately 3000 unique mRNA molecules. To determine the *total* number of  
 397 mRNA that need to be synthesized over the cell's lifetime, we must consider the stability of the  
 398 mRNA. In most bacteria, mRNAs are rather unstable with life times on the order of several min-  
 399 utes per mRNA (BNID: 104324; 106253; 111927; 111998, ?). For convenience, we will assume that  
 400 the typical mRNA in our cell of interest has a typical lifetime of  $\approx 200$  seconds. Using this value, we  
 401 can determine the total mRNA production rate to maintain a steady-state copy number of 3000  
 402 mRNA per cell. While we direct the reader to the appendix to see a derivation of this principle,  
 403 we state here that this production rate must be on the order of  $\approx 15$  mRNA made every second.  
 404 In *E. coli*, the average protein is  $\approx 300$  amino acids in length (BNID: 108986, ?), meaning that the  
 405 corresponding mRNA is  $\approx 900$  nucleotides which we will further approximate to be  $\approx 1000$  nu-  
 406 cleotides given non-protein coding regions of the mRNA present on the 5' and 3' ends. This means  
 407 that the cell must have enough RNA polymerase molecules about to sustain a transcription rate  
 408 of  $\approx 1.5 \times 10^4$  nucleotides per second. Knowing that a single RNA polymerase polymerizes RNA at  
 409 a clip of 40 nucleotides per second, we arrive at a comfortable estimate of  $\approx 250$  RNA polymerase  
 410 complexes needed to satisfy the mRNA demands of the cell. It is worth noting that this number is  
 411 approximately half of that required to synthesize enough rRNA, as we saw in the previous section.  
 412 We find this to be a striking result as these 250 RNA polymerase molecules are responsible for the  
 413 transcription of the  $\approx 4000$  protein coding genes which are not ribosome associated.

### 414 tRNA

415 Our final class of RNA molecules worthy of quantitative consideration is the the pool of tRNAs  
 416 used during translation to map codon sequence to amino acid identity. Unlike mRNA or rRNA,  
 417 each individual tRNA is remarkably short, ranging from 70 to 95 nucleotides each (BNID: 109645;  
 418 102340, ?). What they lack in length, they make up for in abundance. There are approximately  $\approx$   
 419 3000 tRNA molecules present for each of the 20 amino acids (BNID: 105280, ?), although the precise  
 420 copy number is dependent on the identity of the amino acid identity. Using these values, we make  
 421 the estimate that  $\approx 5 \times 10^6$  nucleotides are sequestered in tRNA per cell. Using a similar approach  
 422 as for our estimate of mRNA copy number, the cell requires  $\approx 20$  RNA polymerases to polymerase  
 423 these nucleotides in a 6000 second time window. This requirement pales in comparison to the

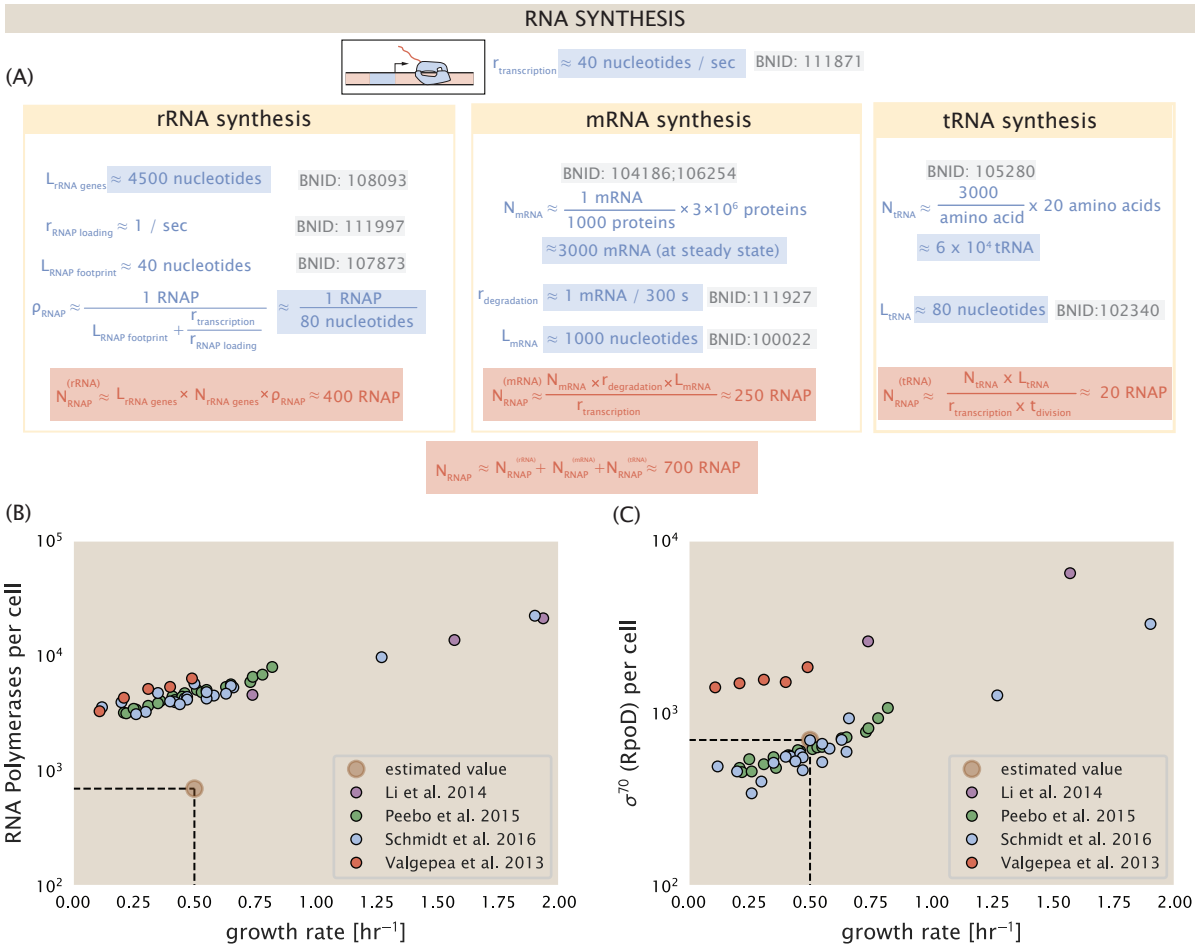


**Figure 7. Estimation of the RNA polymerase abundance and comparison with experimental data.**

424 number of polymerases needed to generate the rRNA pool.

#### 425 RNA Polymerase and $\sigma$ -factor Abundance

426 These estimates, summarized in **Figure 7 (A)**, reveal that synthesis of rRNA is the dominant force  
427 dictating the number of RNA polymerases needed per cell. For completeness, we can use our  
428 estimates of  $\approx 400$ ,  $250$ , and  $20$  RNA polymerases needed to synthesize the required number of  
429 rRNAs, mRNAs, and tRNAs, respectively, to state that the typical cell needs to maintain a pool of  
430  $\approx 700$  RNA polymerases. As is revealed in **Figure 7 (B)**, this estimate is about and an order of  
431 magnitude below the observed number of RNA polymerase complexes per cell ( $\approx 5000$  -  $7000$ ).

432 This disagreement between the estimated number of transcriptionally active RNA polymerases  
433 and these observations jibes with recent literature revealing that  $\approx 80\%$  of RNA polymerases in *E.*  
434 *coli* are not transcriptionally active (?). This leads us to consider other factors intimately involved  
435 in transcription may set the scale of this curious balance.

436 One such factor we can consider is the influence of  $\sigma$ -factors, namely  $\sigma^{70}$  (RpoD) which is the  
437 dominant "general-purpose"  $\sigma$ -factor in *E. coli*. While initially thought of as being solely involved in  
438 transcriptional initiation, the past two decades of single-molecule experimentation has revealed  
439 a more multipurpose role for  $\sigma^{70}$  including facilitating transcriptional elongation (?????). ?? (B) is  
440 suggestive of such a role as the number of  $\sigma^{70}$  proteins per cell is in close agreement with our  
441 estimate of the number of transcriptional complexes needed. In the appendix and supplemental  
442 figure XXX [GC: format number later], the slope of the  $\sigma^{70}$  abundance as a factor of the growth rate

443 can be very accurately estimated by factoring in a) the growth-rate dependent size of the proteome  
 444 and b) the rRNA gene dosage resulting from parallelized replication of the chromosome.

445 While these estimates and comparison with experimental data reveal an interesting dynamic at  
 446 play between the transcriptional demand and copy numbers of the machinery, these findings illus-  
 447 trate that transcription cannot be the rate limiting step in bacterial division. **Figure 7(A)** reveals that  
 448 the availability of RNA polymerase is not limiting as there is ~ 10-fold more complexes than needed.  
 449 Furthermore, if more transcriptional activity was needed to satisfy the cellular requirements, more  
 450  $\sigma^{70}$ -factors could be expressed to utilize more of the pool of RNA polymerase pool.

## 451 Protein synthesis

452 Lastly, we turn our attention to the process of translation. So far in our various estimates there  
 453 has been little to suggest any apparent limit to how fast a bacterium might divide under steady-  
 454 state growth. Even in our examples of *E. coli* grown rapidly under different carbohydrate sources  
 455 (**Figure 2(B)**), cells are able to utilize less preferred carbon sources by inducing the expression of  
 456 additional membrane transporters and enzymes. [Maybe go into Hwa style resource allocation  
 457 with references added]. In this respect, gross overexpression of a protein can lead to a reduction  
 458 of the growth rate.

459 We can determine the translation-limited growth rate by noting that the total number of peptide  
 460 bonds created as the cell doubles  $N_{aa}$  will be given by,  $\tau \cdot r_t \cdot R$ . Here,  $\tau$  refers to the doubling time of  
 461 the cell under steady-state growth,  $r_t$  is the maximum translation rate, and  $R$  is the average number  
 462 of ribosomes in the cell. With the growth rate related to the cell doubling time by  $\lambda = \ln(2)/\tau$ , we  
 463 can write the translation-limited growth rate as,

$$\lambda_{\text{translation-limited}} = \frac{\ln(2) \cdot r_t \cdot R}{N_{aa}}. \quad (1)$$

464 Alternatively, since  $N_{aa}$  is related to the total protein mass through the molecular weight of each  
 465 protein, we can also consider the growth rate in terms of ribosomal mass fraction. This calculation  
 466 is shown in **Figure 8(A)**. This allows us to rewrite the growth rate as,

$$\lambda_{\text{translation-limited}} \approx \frac{\ln(2) \cdot r_t}{L_R} \Phi_R, \quad (2)$$

467 where  $L_R$  is the total length in amino acids that make up a ribosome, and  $\Phi_R$  is the ribosomal mass  
 468 fraction. This is plotted as a function of ribosomal fraction  $\Phi_R$  in **Figure 8(A)**, with a translation rate  
 469  $r_t = 17 \text{ aa/s}$  and  $L_R = 10^6 \text{ aa}$ , which corresponds to the length in amino acids for all ribosomal subunits  
 470 of the 50S and 30S complexes and elongation factor required for translation.

471 Perhaps the first thing to notice is that there is a maximum growth rate at about  $\lambda \approx 6 \text{ hr}^{-1}$ , or  
 472 doubling time of about 7 minutes. This maximum growth rate can be viewed as an inherent speed  
 473 limit due to the need for the cell to double the cell's entire ribosomal mass. Interestingly, this limit is  
 474 independent of the absolute number of ribosomes, but rather is simply given by time to translate  
 475 an entire ribosome,  $L_R/r_t$ . As shown in **Figure 8(B)**, we can reconcile this with the observation  
 476 that in order to double the average number of ribosomes, each ribosome must produce a second  
 477 ribosome. This is a process that cannot be parallelized further.

478 Since a cell consists of more than just ribosomes, we can see that for  $\Phi_R$  in the range of about  
 479 0.1 - 0.3, the maximum growth rate is in line with experimentally reported growth rates around  
 480 0.5 - 2  $\text{hr}^{-1}$ . Here we have implicitly assumed that translation proceeds randomly, without pref-  
 481 erence between ribosomal or non-ribosomal mRNA, which appears reasonable. Importantly, in  
 482 order for a cell to scale this limit set by  $\Phi_R$  the cell must increase its ribosomal abundance, either  
 483 by synthesizing more ribosomes or reducing the fraction of non-ribosomal proteins.

484 One additional point to note is that across different species of bacteria, cells do not decrease  
 485 their ribosomal abundance to zero in the limit of poorer nutrient condition [CITE?]. Indeed, some  
 486 organisms appear to have constant ribosomal abundance irrespective of their growth rate [NB:

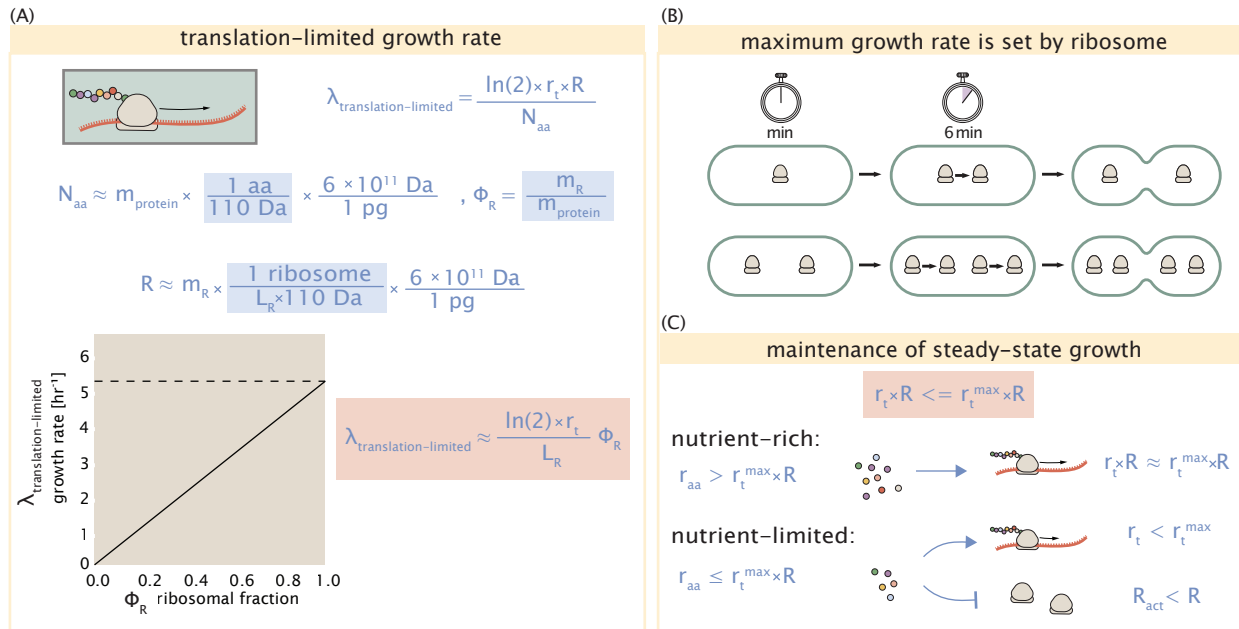


**Figure 8. Translation-limited growth rate.** (A) Here we consider the translation-limited growth as a function of ribosomal fraction. By mass balance, the time required to double the entire proteome ( $N_{\text{aa}} / r_t$ ) sets the translation-limited growth rate,  $\lambda_{\text{translation-limited}}$ . Here  $N_{\text{aa}}$  is effectively the number of peptide bonds that must be translated,  $r_t$  is the translation elongation rate, and  $R$  is the number of ribosomes. This can also be re-written in terms of the ribosomal mass fraction  $\Phi_R = m_R / m_{\text{protein}}$ , where  $m_R$  is the total ribosomal mass and  $m_{\text{protein}}$  is the mass of all proteins in the cell.  $L_R$  refers to the summed length of the ribosome in amino acids.  $\lambda_{\text{translation-limited}}$  is plotted as a function of  $\Phi_R$  (solid line). (B) The dashed line in part (A) identifies a maximum growth rate that is set by the ribosome. Specifically, this growth rate corresponds to the time required to translate an entire ribosome,  $L_R / r_t$ . This is a result that is independent of the number of ribosomes in the cell as shown schematically here. (C)

**Figure 9. . (A) (B) (C).**

ask Griffin and figure out what organism this is]. From the perspective of a bacterium dealing with uncertain nutrient conditions, there is likely a benefit for the cell to maintain some relative fraction of ribosomes to support rapid growth as nutrient conditions improve. In addition, given their massive size at about 850 kDa, they may play an as-yet fully understood role as a crowding agent in cellular function ?? If we consider a scenario where nutrient conditions become poorer and poorer, there must be a regime where the cell has more ribosomes than it can utilize. While this perhaps suggests less import to the process of translation, it is important to recognize that in order for a cell to maintain steady-state growth, the cell's translation capacity must be mitigated. Otherwise, ribosomes will deplete their supply of amino acids and this will bring translation and cell growth to a halt (*Figure 8(C)*). We will consider the consequences of this in the case of *E. coli* next.

#### **498     Multiple replication forks provide one strategy to support faster growth.**

499     We now turn to our proteomic data from *E. coli* and plot the ribosomal fraction as a function of  
500     reported growth rate. Here we find that the ribosomal fraction always increases with growth rate.  
501     This is consistent with the behavior expected for *E. coli*, and an observation of intense study related  
502     to the so-called nutrient-limited growth law. In terms of absolute ribosomal abundance, we find  
503     that cells increase both their quantity and cellular concentration at faster growth.

504     One feature of *E. coli*, as well as other bacteria like *B. subtilis*, is the ability to begin replication of  
505     multiple copies of its genome during a single cell cycle. This is achieved through multiple initiation  
506     forks and nested DNA replication. [need to refer to work from Jun lab here!! - under adder  
507     mechanism, the cell appears to add a certain cell mass in proportion to its number of origins]. We  
508     find that the ribosome copy number increases in proportion to the expected number of origins.  
509     The process of nested DNA replication will lead to a bias in gene dosage for genes closer to the  
510     origin of replication () Importantly, ribosomal protein and rRNA genes are closer to the origin of  
511     replication ? and this provides a natural way for *E. coli* to bias the proportion of ribosomes at faster  
512     growth without the advent of additional gene regulation strategies. Given that ribosomal genes  
513     in *E. coli* appear to be transcribed at their maximal rate at fast growth rates [cite??], increasing  
514     ribosomal copy number through increased gene dosage represents a creative approach for the  
515     cell to grow faster without gross down-regulation of non-ribosomal genes.

#### **516     References**

- 517     Aidelberg, G., Towbin, B. D., Rothschild, D., Dekel, E., Bren, A., and Alon, U. (2014). Hierarchy of non-glucose  
518     sugars in *Escherichia coli*. *BMC Systems Biology*, 8(1):133.
- 519     Antonenko, Y. N., Pohl, P., and Denisov, G. A. (1997). Permeation of ammonia across bilayer lipid membranes  
520     studied by ammonium ion selective microelectrodes. *Biophysical Journal*, 72(5):2187–2195.
- 521     Ashburner, M., Ball, C. A., Blake, J. A., Botstein, D., Butler, H., Cherry, J. M., Davis, A. P., Dolinski, K., Dwight, S. S.,  
522     Eppig, J. T., Harris, M. A., Hill, D. P., Issel-Tarver, L., Kasarskis, A., Lewis, S., Matese, J. C., Richardson, J. E.,  
523     Ringwald, M., Rubin, G. M., and Sherlock, G. (2000). Gene Ontology: tool for the unification of biology. *Nature  
524     Genetics*, 25(1):25–29.
- 525     Ason, B., Bertram, J. G., Hingorani, M. M., Beechem, J. M., O'Donnell, M., Goodman, M. F., and Bloom, L. B.  
526     (2000). A Model for *Escherichia coli* DNA Polymerase III Holoenzyme Assembly at Primer/Template Ends:  
527     DNA Triggers A Change In Binding Specificity of the  $\gamma$  Complex Clamp Loader. *Journal of Biological Chemistry*,  
528     275(4):3006–3015.
- 529     Assentoft, M., Kaptan, S., Schneider, H.-P., Deitmer, J. W., de Groot, B. L., and MacAulay, N. (2016). Aquaporin 4  
530     as a NH<sub>3</sub> Channel. *Journal of Biological Chemistry*, 291(36):19184–19195.
- 531     Basan, M., Zhu, M., Dai, X., Warren, M., Sévin, D., Wang, Y.-P., and Hwa, T. (2015). Inflating bacterial cells by  
532     increased protein synthesis. *Molecular Systems Biology*, 11(10):836.

- 533 Bauer, S. and Ziv, E. (1976). Dense growth of aerobic bacteria in a bench-scale fermentor. *Biotechnology and*  
 534 *Bioengineering*, 18(1):81–94. \_eprint: <https://onlinelibrary.wiley.com/doi/pdf/10.1002/bit.260180107>.
- 535 Belliveau, N. M., Barnes, S. L., Ireland, W. T., Jones, D. L., Sweredoski, M. J., Moradian, A., Hess, S., Kinney, J. B.,  
 536 and Phillips, R. (2018). Systematic approach for dissecting the molecular mechanisms of transcriptional  
 537 regulation in bacteria. *Proceedings of the National Academy of Sciences*, 115(21):E4796–E4805.
- 538 Birnbaum, L. S. and Kaplan, S. (1971). Localization of a Portion of the Ribosomal RNA Genes in *Escherichia coli*.  
 539 *Proceedings of the National Academy of Sciences*, 68(5):925–929.
- 540 Booth, I. R., Mitchell, W. J., and Hamilton, W. A. (1979). Quantitative analysis of proton-linked transport systems.  
 541 The lactose permease of *Escherichia coli*. *Biochemical Journal*, 182(3):687–696.
- 542 Cox, G. B., Newton, N. A., Gibson, F., Snoswell, A. M., and Hamilton, J. A. (1970). The function of ubiquinone in  
 543 *Escherichia coli*. *Biochemical Journal*, 117(3):551–562.
- 544 Delarue, M., Brittingham, G. P., Pfeffer, S., Surovtsev, I. V., Pinglay, S., Kennedy, K. J., Schaffer, M., Gutierrez,  
 545 J. I., Sang, D., Poterewicz, G., Chung, J. K., Plitzko, J. M., Groves, J. T., Jacobs-Wagner, C., Engel, B. D., and Holt,  
 546 L. J. (2018). mTORC1 Controls Phase Separation and the Biophysical Properties of the Cytoplasm by Tuning  
 547 Crowding. *Cell*, 174(2):338–349.e20.
- 548 Escalante, A., Salinas Cervantes, A., Gosset, G., and Bolívar, F. (2012). Current knowledge of the *Escherichia coli*  
 549 phosphoenolpyruvate–carbohydrate phosphotransferase system: Peculiarities of regulation and impact on  
 550 growth and product formation. *Applied Microbiology and Biotechnology*, 94(6):1483–1494.
- 551 Feist, A. M., Henry, C. S., Reed, J. L., Krummenacker, M., Joyce, A. R., Karp, P. D., Broadbelt, L. J., Hatzimanikatis,  
 552 V., and Palsson, B. Ø. (2007). A genome-scale metabolic reconstruction for *Escherichia coli* K-12 MG1655 that  
 553 accounts for 1260 ORFs and thermodynamic information. *Molecular Systems Biology*, 3(1):121.
- 554 Fijalkowska, I. J., Schaaper, R. M., and Jonczyk, P. (2012). DNA replication fidelity in *Escherichia coli*: A multi-DNA  
 555 polymerase affair. *FEMS Microbiology Reviews*, 36(6):1105–1121.
- 556 Gama-Castro, S., Salgado, H., Santos-Zavaleta, A., Ledezma-Tejeida, D., Muñiz-Rascado, L., García-Sotelo, J. S.,  
 557 Alquicira-Hernández, K., Martínez-Flores, I., Pannier, L., Castro-Mondragón, J. A., Medina-Rivera, A., Solano-  
 558 Lira, H., Bonavides-Martínez, C., Pérez-Rueda, E., Alquicira-Hernández, S., Porrón-Sotelo, L., López-Fuentes,  
 559 A., Hernández-Koutoucheva, A., Moral-Chávez, V. D., Rinaldi, F., and Collado-Vides, J. (2016). RegulonDB  
 560 version 9.0: High-level integration of gene regulation, coexpression, motif clustering and beyond. *Nucleic  
 561 Acids Research*, 44(D1):D133–D143.
- 562 Ge, J., Yu, G., Ator, M. A., and Stubbe, J. (2003). Pre-Steady-State and Steady-State Kinetic Analysis of *E. coli* Class  
 563 I Ribonucleotide Reductase. *Biochemistry*, 42(34):10071–10083.
- 564 Goldman, S. R., Nair, N. U., Wells, C. D., Nickels, B. E., and Hochschild, A. (2015). The primary  $\sigma$  factor in *Es-*  
 565 *cherichia coli* can access the transcription elongation complex from solution *in vivo*. *eLife*, 4:e10514.
- 566 Harris, L. K. and Theriot, J. A. (2018). Surface Area to Volume Ratio: A Natural Variable for Bacterial Morphogen-  
 567 esis. *Trends in microbiology*, 26(10):815–832.
- 568 Harris, R. M., Webb, D. C., Howitt, S. M., and Cox, G. B. (2001). Characterization of PitA and PitB from *Escherichia*  
 569 *coli*. *Journal of Bacteriology*, 183(17):5008–5014.
- 570 Heldal, M., Norland, S., and Tumyr, O. (1985). X-ray microanalytic method for measurement of dry matter and  
 571 elemental content of individual bacteria. *Applied and Environmental Microbiology*, 50(5):1251–1257.
- 572 Henkel, S. G., Beek, A. T., Steinsiek, S., Stagge, S., Bettenbrock, K., de Mattos, M. J. T., Sauter, T., Sawodny, O.,  
 573 and Ederer, M. (2014). Basic Regulatory Principles of *Escherichia coli*'s Electron Transport Chain for Varying  
 574 Oxygen Conditions. *PLoS ONE*, 9(9):e107640.
- 575 Hui, S., Silverman, J. M., Chen, S. S., Erickson, D. W., Basan, M., Wang, J., Hwa, T., and Williamson, J. R. (2015).  
 576 Quantitative proteomic analysis reveals a simple strategy of global resource allocation in bacteria. *Molecular  
 577 Systems Biology*, 11(2):e784–e784.
- 578 Ingledew, W. J. and Poole, R. K. (1984). The respiratory chains of *Escherichia coli*. *Microbiological Reviews*,  
 579 48(3):222–271.

- 580 Ireland, W. T., Beeler, S. M., Flores-Bautista, E., Belliveau, N. M., Sweredoski, M. J., Moradian, A., Kinney, J. B.,  
 581 and Phillips, R. (2020). Deciphering the regulatory genome of *Escherichia coli*, one hundred promoters at a  
 582 time. *bioRxiv*.
- 583 Jacob, F. and Monod, J. (1961). Genetic regulatory mechanisms in the synthesis of proteins. *Journal of Molecular  
 584 Biology*, 3(3):318–356.
- 585 Jun, S., Si, F., Pugatch, R., and Scott, M. (2018). Fundamental principles in bacterial physiology - history, recent  
 586 progress, and the future with focus on cell size control: A review. *Reports on Progress in Physics*, 81(5):056601.
- 587 Kapanidis, A. N., Margeat, E., Laurence, T. A., Doose, S., Ho, S. O., Mukhopadhyay, J., Kortkhonjia, E., Mekler, V.,  
 588 Ebright, R. H., and Weiss, S. (2005). Retention of Transcription Initiation Factor  $\Sigma$ 70 in Transcription Elongation:  
 589 Single-Molecule Analysis. *Molecular Cell*, 20(3):347–356.
- 590 Khademi, S., O'Connell, J., Remis, J., Robles-Colmenares, Y., Miercke, L.J. W., and Stroud, R. M. (2004). Mechanism  
 591 of Ammonia Transport by Amt/MEP/Rh: Structure of AmtB at 1.35 Å. *Science*, 305(5690):1587–1594.
- 592 Khademian, M. and Imlay, J. A. (2017). *Escherichia Coli* cytochrome c peroxidase is a respiratory oxidase that  
 593 enables the use of hydrogen peroxide as a terminal electron acceptor. *Proceedings of the National Academy  
 594 of Sciences*, 114(33):E6922–E6931.
- 595 Li, G.-W., Burkhardt, D., Gross, C., and Weissman, J. S. (2014). Quantifying absolute protein synthesis rates  
 596 reveals principles underlying allocation of cellular resources. *Cell*, 157(3):624–635.
- 597 Liu, M., Durfee, T., Cabrera, J. E., Zhao, K., Jin, D. J., and Blattner, F. R. (2005). Global Transcriptional Programs  
 598 Reveal a Carbon Source Foraging Strategy by *Escherichia coli*. *Journal of Biological Chemistry*, 280(16):15921–  
 599 15927.
- 600 Milo, R., Jorgensen, P., Moran, U., Weber, G., and Springer, M. (2010). BioNumbers—the database of key num-  
 601 bers in molecular and cell biology. *Nucleic Acids Research*, 38(suppl\_1):D750–D753.
- 602 Monod, J. (1947). The phenomenon of enzymatic adaptation and its bearings on problems of genetics and  
 603 cellular differentiation. *Growth Symposium*, 9:223–289.
- 604 Mooney, R. A., Darst, S. A., and Landick, R. (2005). Sigma and RNA Polymerase: An On-Again, Off-Again Rela-  
 605 tionship? *Molecular Cell*, 20(3):335–345.
- 606 Mooney, R. A. and Landick, R. (2003). Tethering  $\Sigma$ 70 to RNA polymerase reveals high *in vivo* activity of  $\sigma$  factors  
 607 and  $\Sigma$ 70-dependent pausing at promoter-distal locations. *Genes & Development*, 17(22):2839–2851.
- 608 Neidhardt, F. C., Ingraham, J., and Schaechter, M. (1991). *Physiology of the Bacterial Cell - A Molecular Approach*,  
 609 volume 1. Elsevier.
- 610 Ojkic, N., Serbanescu, D., and Banerjee, S. (2019). Surface-to-volume scaling and aspect ratio preservation in  
 611 rod-shaped bacteria. *eLife*, 8:642.
- 612 Patrick, M., Dennis, P. P., Ehrenberg, M., and Bremer, H. (2015). Free RNA polymerase in *Escherichia coli*.  
*Biochimie*, 119:80–91.
- 614 Peebo, K., Valgepea, K., Maser, A., Nahku, R., Adamberg, K., and Vilu, R. (2015). Proteome reallocation in *Es-*  
*615 cherichia coli* with increasing specific growth rate. *Molecular BioSystems*, 11(4):1184–1193.
- 616 Perdue, S. A. and Roberts, J. W. (2011).  $\sigma^{70}$ -dependent Transcription Pausing in *Escherichia coli*. *Journal of  
 617 Molecular Biology*, 412(5):782–792.
- 618 Phillips, R. (2018). Membranes by the Numbers. In *Physics of Biological Membranes*, pages 73–105. Springer,  
 619 Cham, Cham.
- 620 Ramos, S. and Kaback, H. R. (1977). The relation between the electrochemical proton gradient and active trans-  
 621 port in *Escherichia coli* membrane vesicles. *Biochemistry*, 16(5):854–859.
- 622 Rosenberg, H., Gerdes, R. G., and Chegwidden, K. (1977). Two systems for the uptake of phosphate in *Es-*  
*623 cherichia coli*. *Journal of Bacteriology*, 131(2):505–511.
- 624 Rudd, S. G., Valerie, N. C. K., and Helleday, T. (2016). Pathways controlling dNTP pools to maintain genome  
 625 stability. *DNA Repair*, 44:193–204.

- 626 Sánchez-Romero, M. A., Molina, F., and Jiménez-Sánchez, A. (2011). Organization of ribonucleoside diphosphate  
627 reductase during multifork chromosome replication in *Escherichia coli*. *Microbiology*, 157(8):2220–2225.
- 628 Schaechter, M., MaalØe, O., and Kjeldgaard, N. O. (1958). Dependency on Medium and Temperature of Cell Size  
629 and Chemical Composition during Balanced Growth of *Salmonella typhimurium*. *Microbiology*, 19(3):592–606.
- 630 Schmidt, A., Kochanowski, K., Vedelaar, S., Ahrné, E., Volkmer, B., Callipo, L., Knoops, K., Bauer, M., Aebersold,  
631 R., and Heinemann, M. (2016). The quantitative and condition-dependent *Escherichia coli* proteome. *Nature  
632 Biotechnology*, 34(1):104–110.
- 633 Scholz, S. A., Diao, R., Wolfe, M. B., Fivenson, E. M., Lin, X. N., and Freddolino, P. L. (2019). High-Resolution  
634 Mapping of the *Escherichia coli* Chromosome Reveals Positions of High and Low Transcription. *Cell Systems*,  
635 8(3):212–225.e9.
- 636 Scott, M., Gunderson, C. W., Mateescu, E. M., Zhang, Z., and Hwa, T. (2010). Interdependence of cell growth and  
637 gene expression: origins and consequences. *Science*, 330(6007):1099–1102.
- 638 Sekowska, A., Kung, H.-F., and Danchin, A. (2000). Sulfur Metabolism in *Escherichia coli* and Related Bacteria:  
639 Facts and Fiction. *Journal of Molecular Microbiology and Biotechnology*, 2(2):34.
- 640 Si, F., Le Treut, G., Sauls, J. T., Vadia, S., Levin, P. A., and Jun, S. (2019). Mechanistic Origin of Cell-Size Control  
641 and Homeostasis in Bacteria. *Current Biology*, 29(11):1760–1770.e7.
- 642 Si, F., Li, D., Cox, S. E., Sauls, J. T., Azizi, O., Sou, C., Schwartz, A. B., Erickstad, M. J., Jun, Y., Li, X., and Jun, S. (2017).  
643 Invariance of Initiation Mass and Predictability of Cell Size in *Escherichia coli*. *Current Biology*, 27(9):1278–  
644 1287.
- 645 Sirko, A., Zatyka, M., Sadowy, E., and Hulanicka, D. (1995). Sulfate and thiosulfate transport in *Escherichia coli* K-  
646 12: Evidence for a functional overlapping of sulfate- and thiosulfate-binding proteins. *Journal of Bacteriology*,  
647 177(14):4134–4136.
- 648 Soler-Bistué, A., Aguilar-Pierlé, S., García-Garcérá, M., Val, M.-E., Sismeiro, O., Varet, H., Sieira, R., Krin, E., Skov-  
649 gaard, O., Comerci, D. J., Eduardo P. C. Rocha, and Mazel, D. (2020). Macromolecular crowding links ribosomal  
650 protein gene dosage to growth rate in *Vibrio cholerae*. *BMC Biology*, 18(1):1–18.
- 651 Stasi, R., Neves, H. I., and Spira, B. (2019). Phosphate uptake by the phosphonate transport system PhnCDE.  
652 *BMC Microbiology*, 19.
- 653 Stevenson, B. S. and Schmidt, T. M. (2004). Life History Implications of rRNA Gene Copy Number in *Escherichia  
654 coli*. *Applied and Environmental Microbiology*, 70(11):6670–6677.
- 655 Stouthamer, A. H. and Bettenhausen, C. W. (1977). A continuous culture study of an ATPase-negative mutant  
656 of *Escherichia coli*. *Archives of Microbiology*, 113(3):185–189.
- 657 Szenk, M., Dill, K. A., and de Graff, A. M. R. (2017). Why Do Fast-Growing Bacteria Enter Overflow Metabolism?  
658 Testing the Membrane Real Estate Hypothesis. *Cell Systems*, 5(2):95–104.
- 659 Tatusov, R. L., Galperin, M. Y., Natale, D. A., and Koonin, E. V. (2000). The COG database: a tool for genome-scale  
660 analysis of protein functions and evolution. *Nucleic Acids Research*, 28(1):33–36.
- 661 Taymaz-Nikerel, H., Borjeni, A. E., Verheijen, P. J. T., Heijnen, J. J., and van Gulik, W. M. (2010).  
662 Genome-derived minimal metabolic models for *Escherichia coli* MG1655 with estimated in  
663 vivo respiratory ATP stoichiometry. *Biotechnology and Bioengineering*, 107(2):369–381. \_eprint:  
664 <https://onlinelibrary.wiley.com/doi/pdf/10.1002/bit.22802>.
- 665 The Gene Ontology Consortium (2018). The Gene Ontology Resource: 20 years and still GOing strong. *Nucleic  
666 Acids Research*, 47(D1):D330–D338.
- 667 Valgepea, K., Adamberg, K., Seiman, A., and Vilu, R. (2013). *Escherichia coli* achieves faster growth by increasing  
668 catalytic and translation rates of proteins. *Molecular BioSystems*, 9(9):2344.
- 669 van Heeswijk, W. C., Westerhoff, H. V., and Boogerd, F. C. (2013). Nitrogen Assimilation in *Escherichia coli*: Putting  
670 Molecular Data into a Systems Perspective. *Microbiology and Molecular Biology Reviews*, 77(4):628–695.
- 671 Weber, J. and Senior, A. E. (2003). ATP synthesis driven by proton transport in F1FO-ATP synthase. *FEBS Letters*,  
672 545(1):61–70.

- 673 Willsky, G. R., Bennett, R. L., and Malamy, M. H. (1973). Inorganic Phosphate Transport in Escherichia coli:  
674     Involvement of Two Genes Which Play a Role in Alkaline Phosphatase Regulation. *Journal of Bacteriology*,  
675     113(2):529–539.
- 676 Zhang, L., Jiang, W., Nan, J., Almqvist, J., and Huang, Y. (2014a). The Escherichia coli CysZ is a pH dependent  
677     sulfate transporter that can be inhibited by sulfite. *Biochimica et Biophysica Acta (BBA) - Biomembranes*,  
678     1838(7):1809–1816.
- 679 Zhang, Z., Aboulwafa, M., and Saier, M. H. (2014b). Regulation of crp gene expression by the catabolite repres-  
680     sor/activator, cra, in *Escherichia coli*. *Journal of Molecular Microbiology and Biotechnology*, 24(3):135–141.